

Proceedings of the Fifth Annual LHCP  
ATL-PHYS-PROC-2017-213  
May 7, 2022

## Top pair production in association with a vector gauge boson in ATLAS

JÖRGEN SJÖLIN

*On behalf of the ATLAS Experiment,  
Department of Physics  
Stockholm University, 106 91 Stockholm, Sweden*

### ABSTRACT

An overview of the latest results for top pair production in association with a vector gauge boson in the ATLAS detector at LHC is presented. The results involving  $Z$  and  $W$  bosons are recorded at  $\sqrt{13}$  TeV collision energy, while the results involving photons are recorded at  $\sqrt{7}$  TeV and  $\sqrt{8}$  TeV collision energy.

### PRESENTED AT

The Fifth Annual Conference  
on Large Hadron Collider Physics  
Shanghai Jiao Tong University, Shanghai, China  
May 15-20, 2017

arXiv:1710.05618v1 [hep-ex] 16 Oct 2017

# 1 Introduction

Interactions in the top quark sector are of central interest at the LHC since many new physics scenarios involve top quarks. One example of an important class of scenarios are those that address the Higgs hierarchy problem. For models residing at high energy scales this induces new electroweak top interactions that can be accurately parametrized using effective field theory. Top quark production in association with vector bosons is a strong experimental handle on the leading effective operators that preserve charge-parity and flavour in neutral currents. The experimental input for setting effective theory limits are precision measurements of inclusive and differential cross sections. The latest results from the ATLAS detector [1] in this class of measurements are presented in the following sections.

## 2 Top pairs in association with a $Z$ or $W$ boson

Top quark pairs in associations with heavy vector bosons produce a significant signal in several final states involving leptons, see Figure 1 for the leading significant examples involving  $Z$  and  $W$  bosons. To enhance

Process	$t\bar{t}$ decay	Boson decay	Channel
$t\bar{t}W^\pm$	$(\mu^\pm\nu b)(q\bar{q}b)$	$\mu^\pm\nu$	SS dimuon
	$(\ell^\pm\nu b)(\ell^\mp\nu b)$	$\ell^\pm\nu$	Trilepton
$t\bar{t}Z$	$(\ell^\pm\nu b)(q\bar{q}b)$	$\ell^+\ell^-$	Trilepton
	$(\ell^\pm\nu b)(\ell^\mp\nu b)$	$\ell^+\ell^-$	Tetralepton

Figure 1: List of leading significant final states included in the presented  $t\bar{t}Z$  and  $t\bar{t}W$  analysis.

the sensitivity, each final state is optimized using cuts and then combined to extract the common cross sections using a profile likelihood fit. The resulting cuts from the optimization are shown in Figure 2 for trileptons and in Figure 3 for tetraleptons. The same-sign dimuon events are selected by requiring the muon

Variable	3 $\ell$ -Z-1b4j	3 $\ell$ -Z-2b3j	3 $\ell$ -Z-2b4j	3 $\ell$ -noZ-2b
Leading lepton			$p_T > 25 \text{ GeV}$	
Other leptons			$p_T > 20 \text{ GeV}$	
Sum of lepton charges			$\pm 1$	
Z-like OSSF pair		$ m_{\ell\ell} - m_Z  < 10 \text{ GeV}$		$ m_{\ell\ell} - m_Z  > 10 \text{ GeV}$
$n_{\text{jets}}$	$\geq 4$	3	$\geq 4$	$\geq 2$ and $\leq 4$
$n_{b\text{-jets}}$	1	$\geq 2$	$\geq 2$	$\geq 2$

Figure 2: Summary of event selections in the trilepton signal regions.

transverse momentum  $p_T > 25 \text{ GeV}$ , missing transverse momentum  $E_T^{\text{miss}} > 40 \text{ GeV}$ , the scalar sum of  $p_T$  of leptons and jets ( $H_T$ ) larger than 240 GeV, and at least two b-tagged jets.

The dominating backgrounds vary between the final states. For same-sign leptons non-prompt and fake leptons dominate, in trileptons the  $WZ$  background is large and has significant systematic uncertainties due to extrapolations into the high jet multiplicity signal regions, while in tetraleptons the  $tWZ$  and  $ZZ$  dominate. The diboson backgrounds are estimated by extrapolating the yields from lower jet multiplicity using Monte Carlo, while non-prompt and fake leptons are estimated with the Matrix Method. The Matrix Method parameters are fitted using a Matrix Method likelihood in data control regions, taking into account lepton  $p_T$  and b-tagging multiplicity. Examples of background validation is shown in Figure 4.

An overview of uncertainties affecting the cross section measurement is listed in Table 5, and the measured yields and estimated cross sections are shown in Figure 6.

Region	$Z_2$ leptons	$p_{T34}$	$ m_{Z_2} - m_Z $	$E_T^{\text{miss}}$	$n_{b\text{-tags}}$
4 $\ell$ -DF-1b	$e^\pm\mu^\mp$	$> 35$ GeV	-	-	1
4 $\ell$ -DF-2b	$e^\pm\mu^\mp$	-	-	-	$\geq 2$
4 $\ell$ -SF-1b	$e^\pm e^\mp, \mu^\pm\mu^\mp$	$> 25$ GeV	$\left\{ \begin{array}{l} > 10 \text{ GeV} \\ < 10 \text{ GeV} \end{array} \right.$	$\left\{ \begin{array}{l} > 40 \text{ GeV} \\ > 80 \text{ GeV} \end{array} \right.$	1
4 $\ell$ -SF-2b	$e^\pm e^\mp, \mu^\pm\mu^\mp$	-	$\left\{ \begin{array}{l} > 10 \text{ GeV} \\ < 10 \text{ GeV} \end{array} \right.$	$\left\{ \begin{array}{l} - \\ > 40 \text{ GeV} \end{array} \right.$	$\geq 2$

Figure 3: Summary of event selections in the tetralepton signal regions.

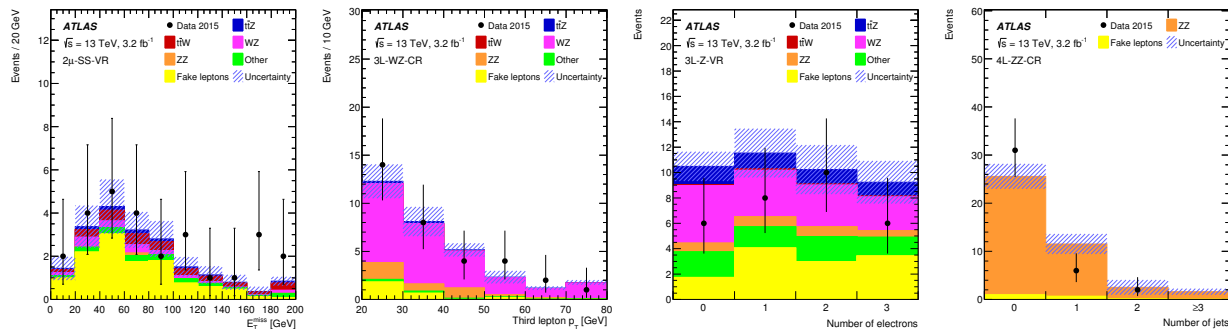


Figure 4: Examples of background validation in the  $t\bar{t}(W/Z)$  measurement [2]. From the left: fakes and non-prompt enhanced event distribution of  $E_T^{\text{miss}}$  in same-sign muons, third leading lepton  $p_T$  in a  $WZ$  enhanced trilepton region, lepton flavor distribution in a trilepton region close to the signal region, and jet multiplicity in a  $ZZ$  enhanced tetralepton region.

### 3 Top pairs in association with a photon

ATLAS has performed measurements of top pairs in association with a photon using data collected at  $\sqrt{s} = 7$  TeV, see Ref. [3]. Preliminary updated and improved results are also available for data collected at  $\sqrt{s} = 8$  TeV, see Ref. [4]. The measurements are performed in a fiducial volume of the detector with photon  $p_T > 20$  GeV (7 TeV data) and photon  $p_T > 15$  GeV (8 TeV data).

The main backgrounds originate from both prompt and non-prompt contributions, and the fractions are determined using a template fit to the photon track isolation within a  $\Delta R \leq 0.2$  cone around the photon. Depending on the process both data and simulations are used to estimate the isolation template shapes.

The prompt photon isolation distribution of the signal is estimated using electrons from  $Z$  boson decays, corrected both for the difference between electrons versus photons and the topology difference between  $Z$  decays and  $t\bar{t}\gamma$  using simulations, in bins of  $p_T$  and pseudo-rapidity ( $\eta$ ).

Contrary to the  $t\bar{t}W$  and  $t\bar{t}Z$  measurements, the  $t\bar{t}\gamma$  measurements are limited by systematic uncertainties, see Table 7 for an overview of the different sources. The measured fractions from signal and different backgrounds after the fit to data are shown in Figure 8. In the updated 8 TeV data measurement, a measurement is also made of the photon differential distributions in  $p_T$  and  $\eta$ , unfolded for detector effects. The differential distributions are shown in Figure 9.

### 4 Conclusions

The production of top pairs with associated bosons is a very active research field at the LHC. The strong interest is partly prompted by the strong ability to constrain EFT operators in the top sector.

Uncertainty	$\sigma_{t\bar{t}Z}$	$\sigma_{t\bar{t}W}$
Luminosity	2.6%	3.1%
Reconstructed objects	8.3%	9.3%
Backgrounds from simulation	5.3%	3.1%
Fake leptons and charge misID	3.0%	19%
Signal modelling	2.3%	4.2%
Total systematic	11%	22%
Statistical	31%	48%
Total	32%	53%

Figure 5: Overview of the systematic uncertainties affecting the  $t\bar{t}(W/Z)$  measurement [2].

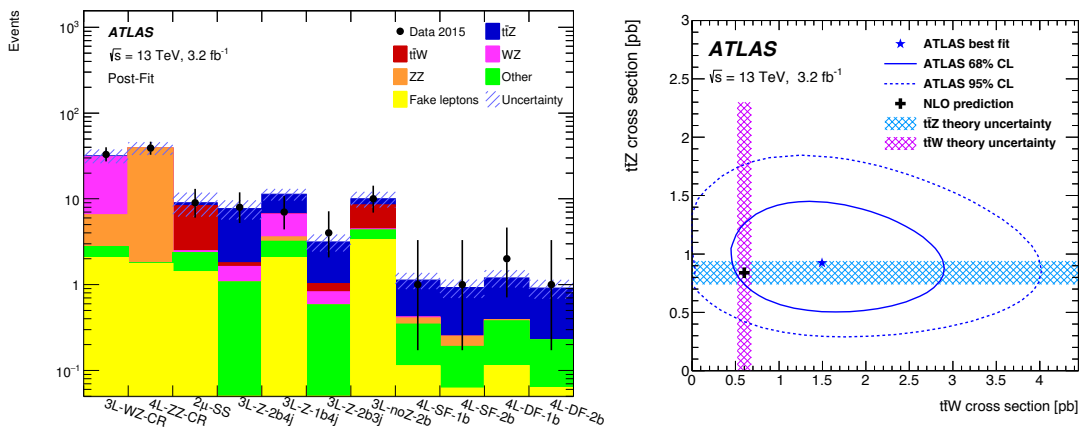


Figure 6: The left plots shows a comparison of the yields in data to expectation in the different regions used in the  $t\bar{t}(W/Z)$  measurement after the fit. On the right a comparison is made between the Standard Model cross section and the simultaneously measured cross sections of  $t\bar{t}W$  and  $t\bar{t}Z$ . The plots are taken from Ref. [2].

Published ATLAS results have been shown for associated  $W$ ,  $Z$  and  $\gamma$  production as well as some new preliminary results of the associated  $\gamma$  production. The focus in the updated measurements are towards making the measurements less model dependent (using well defined fiducial volume) and provide more information beyond just inclusive cross sections, i.e. differential cross sections.

Currently all measured cross sections agree well with the Standard Model predictions. However, the performance of the results are limited by precision, and consequently this kind of measurements will become more and more important in the future as higher statistics LHC data samples become available.

## References

- [1] ATLAS Collaboration, JINST **3** (2008) S08003.
- [2] ATLAS Collaboration, Eur. Phys. J. C **77** (2017) no.1, 40 [arXiv:1609.01599 [hep-ex]].
- [3] ATLAS Collaboration, Phys. Rev. D **91** (2015) no.7, 072007 [arXiv:1502.00586 [hep-ex]].
- [4] ATLAS Collaboration, arXiv:1706.03046 [hep-ex].

Uncertainty source	Uncertainty [%]
Background template shapes	3.7
Signal template shapes	6.6
Signal modeling	8.4
Photon modeling	8.8
Lepton modeling	2.5
Jet modeling	16.6
$b$ -tagging	8.2
$E_T^{\text{miss}}$ modeling	0.9
Luminosity	1.8
Background contributions	7.7

Figure 7: Overview of the systematic uncertainties affecting the 7 TeV data  $t\bar{t}\gamma$  measurement [3].

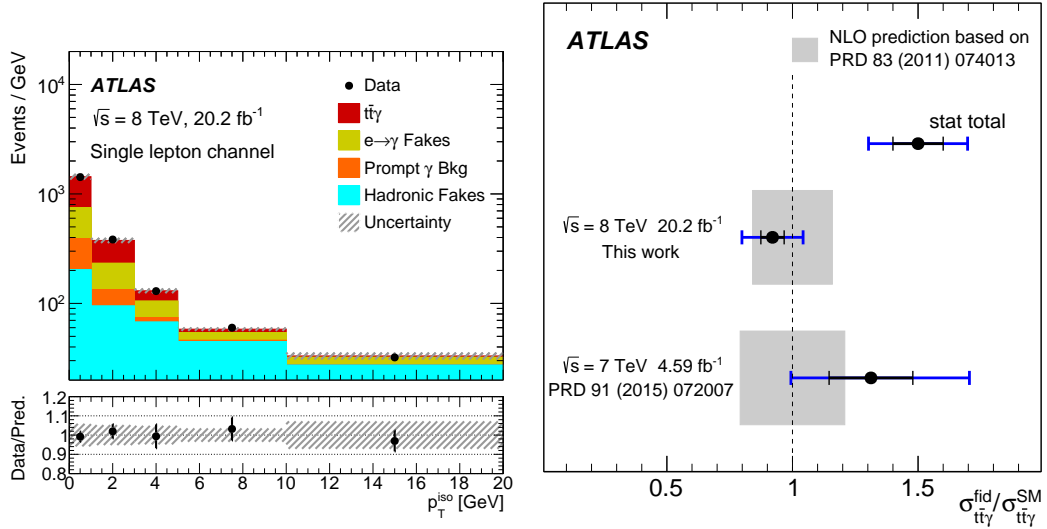


Figure 8: The left plot shows the estimated signal and background fractions after fitting the photon track isolation to data. On the right a comparison is made between the Standard Model prediction of the  $t\bar{t}\gamma$  inclusive cross section and the data measurements, both for the 7 TeV data measurement [3] and the updated 8 TeV data measurement [4].

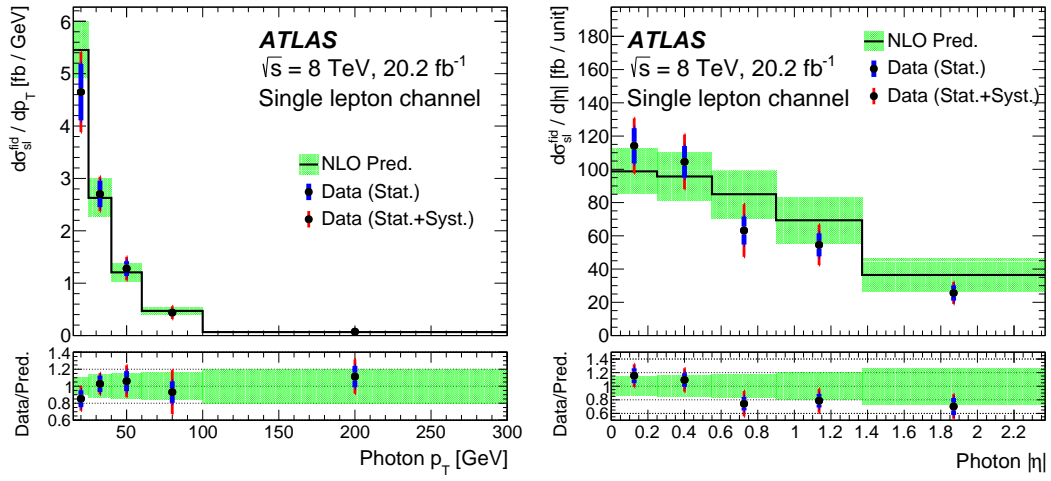


Figure 9: The plots show the detector unfolded differential distributions of the photon  $p_T$  (left) and photon  $\eta$  (right) estimated in the 8 TeV data  $t\bar{t}\gamma$  measurement [4].